Available on CMS information server

CMS CR -2015/031

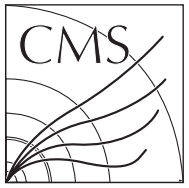

The Compact Muon Solenoid Experiment

Conference Report

Mailing address: CMS CERN, CH-1211 GENEVA 23, Switzerland

13 April 2015 (v2, 29 June 2015)

Measurement of the underlying event activity using charged-particle jets in proton-proton collisions at $\sqrt{s} = 2.76$ TeV

Wei Yang Wang for the CMS Collaboration

Abstract

A measurement of the underlying event (UE) activity in proton-proton collisions is performed using events with a charged-particle jet produced at central pseudorapidity ($| \eta^{\text{jet}} | < 2$) and with transverse momentum $1 \leq p_{\text{T}}^{\text{jet}} < 100$ GeV. The analysis uses a data sample collected by the CMS experiment at the LHC at a centre-of-mass energy of 2.76 TeV, corresponding to an integrated luminosity of 0.3 nb^{-1}. The UE activity is measured as a function of $p_{\text{T}}^{\text{jet}}$ in terms of the average multiplicity and scalar-p_{T} sum of charged particles, with $| \eta | < 2$ and $p_{\text{T}} > 0.5$ GeV, in the azimuthal region transverse to the highest-p_{T} jet direction. By further dividing the transverse region into two halves of smaller and larger activity respectively, valuable information on different UE contributions is obtained. The measurements are compared to previous results at 0.9 and 7 TeV, and to predictions of several Monte Carlo event generators, providing constraints on the theoretical modelling of the UE dynamics.

Presented at *MassiveNeutrinos International Conference on Massive Neutrinos*

Measurement of the underlying event activity using charged-particle jets in proton-proton collisions at $\sqrt{s} = 2.76$ TeV

W. Y. Wang*, A. H. Chan and C. H. Oh

On behalf of the CMS Collaboration

Department of Physics, National University of Singapore, Singapore

* *E-mail: w.y.wang@u.nus.edu*

www.nus.edu.sg

A measurement of the underlying event (UE) activity in proton-proton collisions is performed using events with a charged-particle jet produced at central pseudorapidity ($|\eta^{\rm jet}| < 2$) and with transverse momentum $1 \leq p_{\rm T}^{\rm jet} < 100$ GeV. The analysis uses a data sample collected by the CMS experiment at the LHC at a centre-of-mass energy of 2.76 TeV, corresponding to an integrated luminosity of 0.3 nb^{-1}. The UE activity is measured as a function of $p_{\rm T}^{\rm jet}$ in terms of the average multiplicity and scalar-$p_{\rm T}$ sum of charged particles, with $|\eta| < 2$ and $p_{\rm T} > 0.5$ GeV, in the azimuthal region transverse to the highest-$p_{\rm T}$ jet direction. By further dividing the transverse region into two halves of smaller and larger activity respectively, valuable information on different UE contributions is obtained. The measurements are compared to previous results at 0.9 and 7 TeV, and to predictions of several Monte Carlo event generators, providing constraints on the theoretical modelling of the UE dynamics.

1. Introduction

Hadron production in high-energy proton-proton (pp) collisions originates from multiple scatterings of the partonic constituents of the protons at central rapidities, and from "spectator" (non-colliding) partons emitted in the very forward direction. The produced partons reduce their virtuality through gluon radiation and quark-antiquark splittings, and finally fragment into hadrons at scales approaching $\Lambda_{\rm QCD} \approx 0.2$ GeV. Usually, one separates the produced hadrons into two classes: those directly coming from the fragmentation of partons with the largest momentum transfer ("hard scattering") in the event, and the rest ("underlying event", or UE). The UE, thus, consists of hadrons coming from (i) initial- and final-state radiation (ISR, FSR) from the hard scattering, (ii) softer partonic scatters in the same collision (multiple parton interactions, or MPI), and (iii) beam remnants concentrated along the beam direction.

An accurate understanding of the UE is required for precise measurements of standard model processes at high energies and searches of new physics. Indeed, the UE affects measurements of isolated high-$p_{\rm T}$ leptons or photons, and it dominates most of the hadronic activity from the overlapping "minimum bias" pp collisions taking place in a given bunch crossing at high LHC luminosities. The semihard and low-momentum processes, which dominate the UE, cannot be theoretically de-

scribed with perturbative QCD (pQCD) methods alone, and require a phenomenological description containing parameters that must be tuned to the data.

The topological structure of pp interactions with a hard scattering can be used to define experimental observables which are sensitive to the UE. One example is the study of particle properties in regions away from the direction of the products of the hard scattering. At the Tevatron, the CDF experiment measured UE observables using inclusive jet and Drell–Yan (DY) events in $\mathrm{p\bar{p}}$ collisions at centre-of-mass energies $\sqrt{s}$ = 0.63, 1.8, and 1.96 TeV[1–3]. In pp collisions at the LHC, the CMS, ATLAS, and ALICE experiments have carried out UE measurements at $\sqrt{s}$ = 0.9 and 7 TeV using events containing a leading (highest-p_{T}) charged-particle jet[4,5] or a leading charged particle[6,7], and in DY events[8]. In this paper, we study the UE activity by measuring the average multiplicity and scalar transverse momentum sum (Σp_{T}) densities of charged particles in the azimuthal transverse region with respect to the leading charged particle jet in pp collisions at $\sqrt{s}$ = 2.76 TeV.

At a given centre-of-mass energy, the UE activity is expected to increase with the hard scale of the interaction. On average, increasingly harder parton interactions result from pp collisions with decreasing impact parameters which, in turn, enhance the overall hadronic activity originating from MPI up to a saturation reached for central collisions with maximum overlap[9,10]. At the same time, the activity related to the ISR and FSR components continues to increase with the hard scale. For events with the same hard scale, e.g. given by the p_{T} of jets or DY pairs, the MPI activity rises with $\sqrt{s}$, as denser parton distributions in the protons are probed at increasingly smaller parton fractional momenta $x \sim 2\,p_T/\sqrt{s}$[9,10]. Hence, studying the UE as a function of the hard scale at several centre-of-mass energies provides an insight into the UE dynamics and its evolution with the collision energy, further constraining the model parameters.

The paper is organised as follows. Section 2 presents the main features of the Monte Carlo (MC) event generators used in this study, that are relevant for the description of the UE properties. Section 3 briefly describes the experimental methods, observables, event and track selection, as well as the corrections and systematic uncertainties of the measurements. The results are presented in Section 4, and summarised in Section 5.

2. Monte Carlo event generators

In this analysis, the PYTHIA6[11], PYTHIA8[12], and HERWIG++[13] MC event generators are used, with various tunes that are described below. In PYTHIA, the $2 \to 2$ non-diffractive processes, including multiple partonic interactions, are described by lowest-order perturbative QCD with the divergence of the cross-section as $p_{\mathrm{T}} \to 0$ regulated with a phenomenological model. There are various tunable parameters that control, among other things, the behaviour of this regularisation, the transverse matter profile distribution of partons within the hadrons, and final state colour reconnection effects among the produced partons. When QCD radiation is modelled

via a p_{T}-ordered evolution, the MPI and parton shower are interleaved in one common sequence of decreasing p_{T} values[14]. For the latest version of PYTHIA6, the interleaving is between the initial-state shower and MPI only, while for PYTHIA8 it also includes final-state showers. The final non-perturbative transition of partons to hadrons is described by the Lund string fragmentation model[15].

HERWIG++ is another general purpose generator like PYTHIA, but it uses angular-ordered parton showers and the cluster model[13] for hadronisation. It has an MPI model similar to the one used by PYTHIA, with tunable parameters for regularising the partonic cross sections at low momentum transfer, but does not include the interleaved evolution with ISR and FSR. While HERWIG++ has no explicit model for diffractive interactions, diffractive-like events are simulated by applying the MPI model to events in which only beam remnants are produced, with no other activity between them.

Both MC models incorporate multiple parton collisions "perturbatively"—i.e. based on a "regularisation" of underlying pQCD subprocess cross sections—but require a non-perturbative ansatz for the impact-parameter profile of the colliding protons. MPIs are then generated by assuming a Poissonian distribution of elementary partonic interactions over the overlapping pp volume, with an average number depending on the impact parameter of the hadronic collision[9,10]. The MPI cross section is dominated by scatterings with semi-hard momentum transfers, O(1–2 GeV) in the low-x regime of the parton densities, and thus show a stronger dependence on the incoming parton fluxes than the single hard-scattering interactions[9,10], and on the evolution of the low-p_{T} infrared cutoff, p_{T_0}. In PYTHIA6, PYTHIA8 and HERWIG++, the energy dependence of MPIs is mostly controlled by the energy evolution of the p_{T_0} parameter, which follows a (tunable) power-law dependence on the centre-of-mass energy[11–13]. The dependence of the UE activity on the energy scale is well described by Monte Carlo event generators[4–8], illustrating the universality of MPIs in different event topologies and hard-scattering production processes. Such a universality is confirmed by the similarity between the UE activity measured in DY[8] and jet-dominated events[4–7], despite their different underlying parton radiation patterns.

In this analysis, several event generators tunes are used for comparison with the data. These are the PYTHIA6 version 6.426[11] tune Z2*[16] and tune CUETP6S1[17], PYTHIA8 version 8.175 [12] tune 4C[18] and CUETP8S1[17], and HERWIG++ 2.7 tune UE-EE-5C[13,19]. These event generators and tunes differ in the treatment of initial- and final-state radiation, hadronisation, colour reconnections, and cutoff values for the MPI mechanism. These tunes were mostly obtained from comparisons between predictions and data aimed at providing a reasonable description of existing UE data, especially those measured from LHC pp collisions. In addition, minimum bias observables measured at lower (Tevatron) energies were also used.

3. Experimental methods

The central feature of the CMS apparatus is a superconducting solenoid of 6 m internal diameter, providing a magnetic field of 3.8 T. Within the superconducting solenoid volume there are several complementary detectors: a silicon pixel and strip tracker, a lead tungstate crystal electromagnetic calorimeter, and a brass/scintillator hadron calorimeter, each composed of a barrel and two endcap sections. The silicon tracker measures charged particles within the pseudorapidity range $|\eta| < 2.5$. For non-isolated particles of $1 < p_{\mathrm{T}} < 10$ GeVand $|\eta| < 1.4$, the track resolutions are typically 1.5% in p_{T}, and 25–90 (45–150) μm in the transverse (longitudinal) impact parameter[20]. Two of the CMS subdetectors acting as LHC beam monitors, the Beam Scintillation Counters (BSC) and the Beam Pick-up Timing for the eXperiments (BPTX) devices, were used to trigger the detector readout. The BSC are located along the beam line on each side of the IP at a distance of 10.86 m and cover the pseudorapidity range $3.23 < |\eta| < 4.65$. The two BPTX devices, located inside the beam pipe at distances of 175 m from the IP, are designed to provide precise information on the bunch structure and timing of the incoming beams, with a time resolution better than 0.2 ns. A more detailed description of the CMS detector, together with a definition of the coordinate system used and the relevant kinematic variables, can be found in Ref. 21.

3.1. *Observables*

In this analysis we follow the same methodology as in the previous studies of the UE activity in events with a leading charged-particle jet, carried out at $\sqrt{s} =$ 0.9 and 7 TeV[4]. Charged-particle jets and charged particles produced at central pseudorapidity ($|\eta| < 2$) with transverse momentum larger than 1 GeVand 0.5 GeV, respectively, are used to study the UE properties. The direction of the leading charged-particle jet in the event is used to select charged particles in the azimuthal transverse region defined by $60^\circ < |\Delta\phi| < 120^\circ$, where $\Delta\phi$ is the relative azimuthal distance between a charged particle and the leading jet. The UE is measured in terms of particle and Σp_{T} densities as a function of the leading jet transverse momentum $p_{\mathrm{T}}^{\mathrm{jet}}$, which is used as a proxy for the hard scale of the interaction. The particle density ($\langle N_{\mathrm{ch}} \rangle \,/\, [\Delta\eta\Delta(\Delta\phi)]$) and Σp_{T} density ($\langle \sum p_{\mathrm{T}} \rangle \,/\, [\Delta\eta\Delta(\Delta\phi)]$) are computed, respectively, as the average number of primary charged particles, and the average of the scalar sum of their transverse momenta, each per unit of η and per unit of $\Delta\phi$.

As suggested in Ref. 22, the transverse region can be studied in more detail by separating —independently for the particle multiplicity and for the p_{T} sum— the $60^\circ < \Delta\phi < 120^\circ$ and the $-120^\circ < \Delta\phi < -60^\circ$ ranges, and identifying the region with higher and lower activity, as transMAX and transMIN, respectively. The difference between the transMAX and transMIN activities is used to construct the transDIF activity. The resulting particle and Σp_{T} densities are expected to be sensitive to different components of the UE activity.

For events with large initial- or final-state radiation, the transMAX region contains the third jet, while both transMAX and transMIN regions receive contributions from the MPI and beam remnants. The transMIN activity is therefore sensitive to MPI and beam remnants, and the transDIF activity is sensitive to harder initial- and final-state radiation. Such an approach extends the methodology employed in Ref. 4.

3.2. *Event and track selection*

The present analysis is performed with a data sample of proton-proton collisions collected by the CMS detector at $\sqrt{s} = 2.76$ TeVduring a dedicated run in March 2011, corresponding to an integrated luminosity of 0.3 nb^{-1}. In 6.2% of the events, there is an extra (pileup) pp collision, corresponding to an average of 0.12 overlapping pp collisions. Minimum bias events were recorded by requiring activity in both BSC counters in coincidence with signals from both BPTX devices (in contrast to Ref. 4 which requires only one of the BPTX devices). To reduce the statistical uncertainty for large $p_{\mathrm{T}}^{\mathrm{jet}}$, jet triggers based on information from the calorimeters, with p_{T} thresholds at 20 and 40 GeV, were also used to collect data (at variance with Ref. 4 which uses thresholds of 30 and 50 GeV). Events identified as originating from beam-halo background are removed from the triggered events[23]. Event selection requires exactly one primary vertex with more than four degrees of freedom and no more than ± 10 cm from the centre of the luminous region (beamspot) in the z-direction.

For each selected event the reconstructed track collection needs to be cleaned up from undesired tracks, namely secondaries and background from track combinatorics and beam halo associated tracks.. Tracks not corresponding to actual charged particles (fake tracks) are reduced by imposing the *highPurity* selection criteria[20]. Secondary decays are reduced by requiring that the impact parameter significance $d_0/\sigma(d_0)$ and the significance of z separation between the track and primary vertex $d_z/\sigma(d_z)$, to be each less than 3. In order to remove tracks with poor momentum measurement, we require the calculated relative uncertainty of the momentum measurement $\sigma(p_{\mathrm{T}})/p_{\mathrm{T}}$ to be less than 5%. Average reconstruction efficiency for the selected tracks is about 85%, which drops to 75% for low p_{T} tracks and large η, while the fake track rate is about 2%, increasing for tracks with small p_{T} or large $|\eta|$.

The event energy scale and reference direction, for the identification of the UE sensitive region, are defined using leading "track jets"[24]. The track jets used in this study are reconstructed from charged-particle tracks with $p_{\mathrm{T}} > 0.5$ GeV and $|\eta| < 2.5$ using the SISCone[25] algorithm with distance parameter of 0.5. Although anti-$\mathrm{k_T}$[26] is now the most preferred algorithm at the LHC, the SISCone algorithm is chosen in this analysis for compatibility with previous results[4]. A comparison of the UE activity obtained at generator level using SISCone and anti-$\mathrm{k_T}$[26] algorithms was performed, finding only few percent differences at low $p_{\mathrm{T}}^{\mathrm{jet}}$. From all reconstructed

track jets with $|\eta| < 2$ and $p_{\mathrm{T}} > 1.0$ GeV, the one with largest $p_{\mathrm{T}}^{\mathrm{jet}}$ is selected. Events without such a jet are not considered in the analysis. Jets are reconstructed with a matching efficiency of 80% at the lowest $p_{\mathrm{T}}^{\mathrm{jet}}$ and up to 95% for $p_{\mathrm{T}}^{\mathrm{jet}} > 20$ GeV. Trigger conditions are matched to keep the efficiency as uniform as possible and close to 100%. For $1 < p_{\mathrm{T}}^{\mathrm{jet}} < 25$ GeV, $25 < p_{\mathrm{T}}^{\mathrm{jet}} < 50$ GeV, and $p_{\mathrm{T}}^{\mathrm{jet}} > 50$ GeV, we use respectively the minimum-bias and the two-jet triggered samples, corresponding to about 11M, 50k and 23k finally selected events.

3.3. *Corrections and systematic uncertainties*

The UE observables ($\langle N_{\mathrm{ch}} \rangle / [\Delta\eta\Delta(\Delta\phi)]$and $\langle \sum p_{\mathrm{T}} \rangle / [\Delta\eta\Delta(\Delta\phi)]$) are reconstructed from all selected tracks, with $p_{\mathrm{T}} > 0.5$ GeV and $|\eta| < 2$, in the transverse region to the leading track jet. These measured observables are corrected for detector effects and selections efficiencies to reflect the primary charged-particle activity corresponding to events with the same kinematic properties. An iterative unfolding technique[27] is used based on 4-dimensional response matrices. These matrices are constructed from the UE observables as a function of $p_{\mathrm{T}}^{\mathrm{jet}}$ at (MC generator level) particle and reconstructed levels based on simulated events from the PYTHIA6 Z2 tune, accounting for the response of the observables to detector effects and inefficiencies. An unfolding of the PYTHIA8 4C reconstructed events based on response matrices obtained from Z2 is used to estimate the systematic uncertainties related to the correction procedure. These vary between 1% and 4% depending on the observables and $p_{\mathrm{T}}^{\mathrm{jet}}$.

Several other sources of systematic uncertainties may affect the results. These include the implementation of the simulation of track and vertex selection criteria, tracker alignment and material content, background contamination, trigger conditions, and pileup contributions. The uncertainty in the simulation of track selection has been evaluated by applying various sets of selection criteria and comparing their effects to the data and to simulated events. The impact-parameter significance ranges are varied by one unit around the nominal window resulting in an effect on the densities of 2 to 4%. It has also been checked that replacing the *highPurity* selection by a simple cut of $N_{\mathrm{layers}} \geq 4$ and $N_{\mathrm{pixel\ layers}} \geq 2$ for silicon strip and pixel detector layers respectively, has an effect of only 0.2%. Varying the fraction of fake tracks by 50% affects the densities by 0.4 to 0.5%. The description in the simulation of inactive tracker material has been found to be adequate to within 5%, and increasing the material densities by 5% in the simulation induces a change in the observables of 1%. The effects of tracker misalignment, precision in the interaction point position, and dead channels, evaluated by varying the detector conditions in the MC simulation, are all found to change the results by 0.1 to 0.3%. The effect of varying the trigger and vertex efficiencies within their uncertainties, as well as the effect of pileup contributions, have all been found to lead to a negligible effect.

Systematic uncertainties are largely independent of one another, but they are

correlated among data points in each observable. Table 1 shows a summary of the systematic uncertainties.

Source	Systematic (%)
Unfolding procedure	1–4
Impact parameter signif.	2–4
Fraction of fake tracks	0.4–0.5
Track selection	0.2
Material density	1.0
Dead channels	0.1
Tracker alignment	0.2–0.3
Interaction point position	0.2
Total	2.5–5.8

4. Results

In Fig. 1, the (a) particle and (b) Σp_{T} densities, after unfolding, are shown in the transverse region, relative to the leading charged-particle jet, as a function of the transverse momentum $p_{\mathrm{T}}^{\mathrm{jet}}$. A steep rise of the underlying event activity in the transverse region is seen up to $p_{\mathrm{T}}^{\mathrm{jet}} \sim 8$ GeV, followed by a "saturation" (plateau-like) region, with nearly constant multiplicity and small Σp_{T} density increase. In Fig. 2, the (a)(c) particle and (b)(d) Σp_{T} densities after unfolding are shown as a function of $p_{\mathrm{T}}^{\mathrm{jet}}$ in the transverse region with maximum activity (transMAX) and with minimum activity (transMIN). In the transMIN region, the amount of UE activity is roughly twice smaller compared to transMAX. The shape is also quite different in both categories. At high-p_{T} the distributions show a slow rise in transMAX, while in transMIN the plateau-like region is more pronounced. The corresponding distributions in the difference between the transMAX and transMIN regions (transDIF) are presented in Fig. 3. The particle and Σp_{T} densities both show a rise with $p_{\mathrm{T}}^{\mathrm{jet}}$, and the plateau-like region above $p_{\mathrm{T}}^{\mathrm{jet}} \approx 8$ GeV—seen in the previous transMAX and transMIN distributions—is substituted by less pronounced rises as a function of jet transverse momentum.

The rapid increase of the UE activity with $p_{\mathrm{T}}^{\mathrm{jet}}$ in the region below ~ 8 GeV is mainly attributed to the increase of MPI activity as the scale of the interaction increases[10]. This fast rise is followed by a saturation region, with nearly constant multiplicity and small Σp_{T} density increase. This behaviour is expected in the transverse impact parameter picture, as a consequence of a nearly full overlap of the colliding protons in interactions yielding the hardest parton-parton scatterings. Once the most central pp collisions are reached, the amount of MPI activity saturates[9,10]. Such a distinct $p_{\mathrm{T}}^{\mathrm{jet}}$-dependent pattern in the amount of UE activity (sharp rise plus plateau above the $p_{\mathrm{T}}^{\mathrm{jet}} \approx 8$ GeVtransition) is clearly seen for all the

observables presented in the paper. However the transMAX and transDIF distributions show a continuous rise with $p_{\mathrm{T}}^{\mathrm{jet}}$ also in the high-p_{T} tails. This is expected to be caused by contributions from initial- and final-state radiation in the tranverse region [22]. Assuming such an interpretation, the present results provide valuable constraints on the modelling of the different UE components.

The results are compared to recent tunes of PYTHIA and HERWIG++ event generators. In general, all PYTHIA6 and PYTHIA8 tunes predict the distinctive change of the amount of activity as a function of the leading jet p_{T} within 5–10%. The HERWIG++ UE-EE-5C tune also provides a fair description of the data. In general, the data-model agreement improves in the transDIF region. The continuous increase observed at high-$p_{\mathrm{T}}^{\mathrm{jet}}$ in the transDIF distributions is well reproduced by all MC tunes, corroborating the hypothesis of increased contributions of QCD radiation from the hardest scattered partons. The same trend is observed in Ref. 3. The latest PYTHIA6 (PYTHIA8) tune CUETP6S1 (CUETP8S1) improves the description of the data in comparison to the results obtained with the parameters of the previous Z2* (4C) tunes.

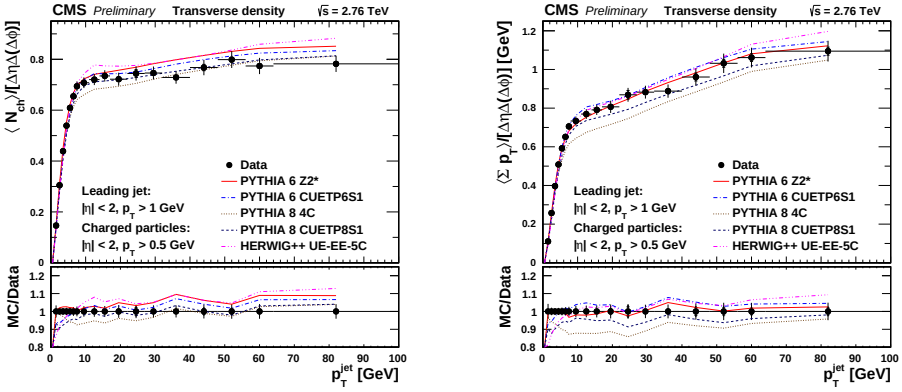

(a) (b)

Fig. 1. Measured (a) particle density, and (b) Σp_{T} density, in the transverse region relative to the leading charged-particle jet in the event ($|\eta| < 2, 60^\circ < |\Delta\varphi| < 120^\circ$), as a function $p_{\mathrm{T}}^{\mathrm{jet}}$. The data (symbols) are compared to various Monte Carlo predictions (curves). The ratios of MC predictions to the measurements are shown in the bottom panels. The inner error bars correspond to the statistical uncertainties, and the outer error bars represent the statistical and systematic uncertainties added in quadrature.

The centre-of-mass energy dependence of the UE activity in the transverse region is presented in Fig. 4 as a function of $p_{\mathrm{T}}^{\mathrm{jet}}$ for $\sqrt{s} = 0.9$, 2.76 and 7 TeV [4,5]. A fast rise with increasing centre-of-mass energy of the activity in the transverse region is observed for the same value of the leading charged-particle jet p_{T}. All tunes predict a centre-of-mass energy dependence of the UE activity, which is very consistent with that found in the data.

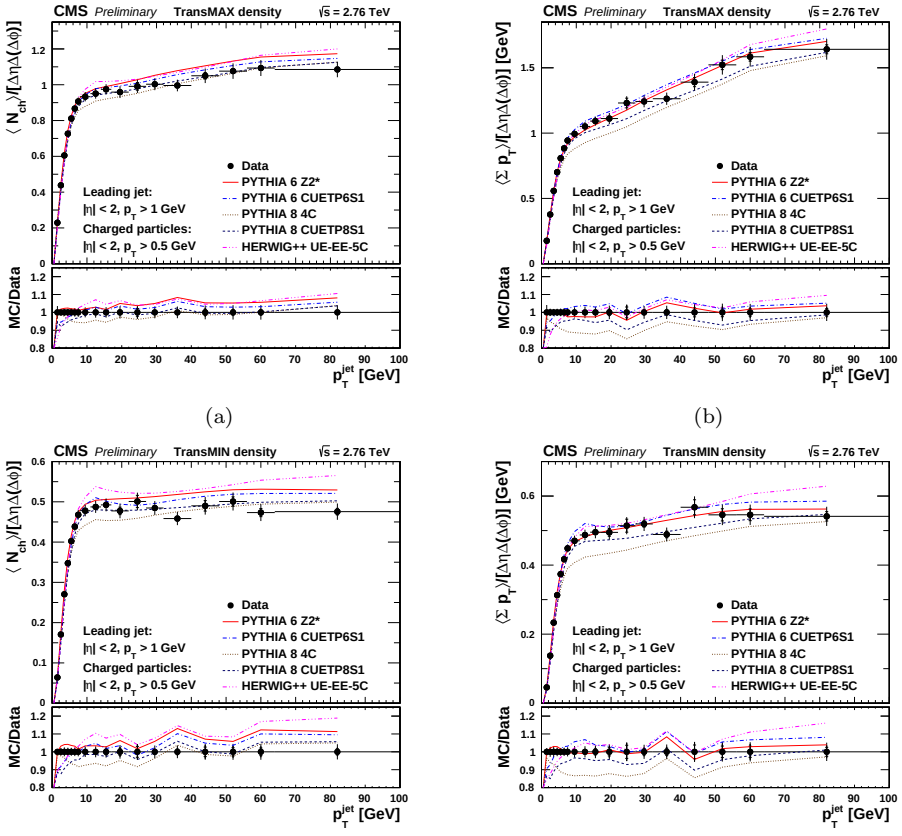

Fig. 2. Measured (a)(c) particle density, and (b)(d) Σp_{T} density, in the transMAX and transMIN region ($60^\circ < |\Delta\varphi| < 120^\circ$, relative to the leading charged-particle jet in the event, with maximum/minimum UE activity), as a function of $p_{\mathrm{T}}^{\mathrm{jet}}$. The definitions of symbols and error bars is the same as Fig. 1.

5. Summary

The measurement of the underlying event (UE) activity in proton-proton collisions at $\sqrt{s} = 2.76$ TeV has been presented using events with a charged-particle jet produced at central pseudorapidity ($|\eta^{\mathrm{jet}}| < 2$) with transverse momenta $1 < p_{\mathrm{T}}^{\mathrm{jet}} < 100$ GeV. Such analysis complements the results of previous similar measurements at $\sqrt{s} = 900$ GeV and 7 TeV.

The leading charged-particle jet in each event is used to set a reference for the energy scale of the hardest partonic scattering, and to define different regions of hadronic activity in azimuth space. The transverse region to the jet's direction is mostly sensitive to UE contributions, and the corresponding charged-hadron activity is studied by measuring its particle and Σp_{T} densities. Furthermore, by

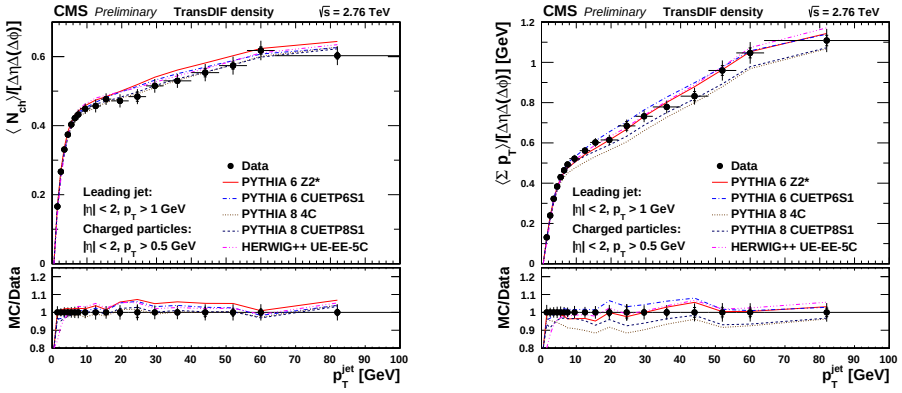

(a) (b)

Fig. 3. Measured transDIF activity (see text for its definition) for (a) particle density, and (b) Σp_{T} density, as a function of $p_{\mathrm{T}}^{\mathrm{jet}}$. The definitions of symbols and error bars is the same as Fig. 1.

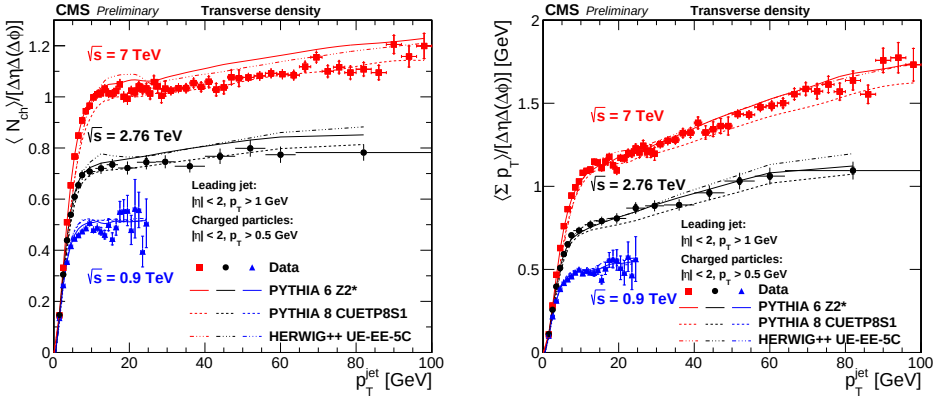

(a) (b)

Fig. 4. Comparison of UE activity at $\sqrt{s} = 0.9$, 2.76, and 7 TeV for (a) particle density, and (b) Σp_{T} density, as a function of $p_{\mathrm{T}}^{\mathrm{jet}}$[4,5]. The data (symbols) are compared to various MC simulations (curves). The definitions of the error bars is the same as Fig. 1.

dividing the transverse region into minimum and maximum activity areas, the UE contributions from initial- and final-state parton radiation (ISR and FSR) from the hardest scatter can be better factorised out from those originating in multiparton interactions (MPI) and "spectator" partons (beam remnants).

A steep rise of the underlying activity in the transverse region is seen with increasing leading jet p_{T}. This is followed by a plateau above $p_{\mathrm{T}}^{\mathrm{jet}} \sim 8$ GeV, with nearly constant multiplicity and small Σp_{T} density increase. The fast rise followed by a plateau of the UE hadronic activity is clearly seen for all the observables, and confirms the impact-parameter picture of pp collisions featuring an increasing

number of MPIs for increasing overlap followed by a saturation of hadron production once the hardest most-central collisions are reached. The transDIF activity shows an increase of the activity with $p_{\mathrm{T}}^{\mathrm{jet}}$ corroborating the hypothesis of a rising contribution from ISR and FSR from the increasingly harder parton-parton scatter.

By comparing data taken at $\sqrt{s}$= 0.9, 2.76, and 7 TeV, a strong growth of the UE activity with higher centre-of-mass energy is observed for the same value of the leading charged-particle $p_{\mathrm{T}}^{\mathrm{jet}}$ as expected from the denser parton densities probed at low-x in the protons, and the larger phase space available for parton radiation.

The results are compared to recent tunes of PYTHIA and HERWIG++ Monte Carlo event generators. PYTHIA6, PYTHIA8 and HERWIG++ tunes describe the data within 5 to 10%. All MC tunes correctly predict the collision-energy dependence of the hadronic activity that is very similar to that observed in the data. The measurements presented here provide valuable constraints for the development and tuning of the underlying event description implemented in hadronic MC models. They will allow one to improve the modelling of key ingredients—such as multiparton interactions, QCD radiation, energy evolution of the transverse proton profile, etc.—which will play an increasing role at higher proton-proton collision energies.

Acknowledgements

We thank our colleagues at CERN, the CMS collaboration and the University of Antwerp for the support given to this work. We are also thankful for the funding provided by Lee Foundation and the NUS Research Grant WBS: R-144-000-178-112.

References

1. T. Affolder *et al.*, Charged jet evolution and the underlying event in proton-antiproton collisions at 1.8 TeV, *Phys. Rev. D* **65**, p. 092002 (2002).
2. D. Acosta *et al.*, Underlying event in hard interactions at the Fermilab Tevatron $\overline{p}p$ collider, *Phys. Rev. D* **70**, p. 072002 (2004).
3. T. Aaltonen *et al.*, Studying the underlying event in Drell-Yan and high transverse momentum jet production at the Tevatron, *Phys. Rev. D* **82**, p. 034001 (2010).
4. S. Chatrchyan *et al.*, Measurement of the underlying event activity at the LHC with $\sqrt{s} = 7$ TeV and comparison with $\sqrt{s} = 0.9$ TeV, *JHEP* **09**, p. 109 (2011).
5. V. Khachatryan *et al.*, First measurement of the underlying event activity at the LHC with $\sqrt{s} = 0.9$ TeV, *Eur. Phys. J. C* **70**, p. 555 (2010).
6. B. Abelev *et al.*, Underlying event measurements in pp collisions at $\sqrt{s} = 0.9$ and 7 TeV with the ALICE experiment at the LHC, *JHEP* **07**, p. 116 (2012).
7. G. Aad *et al.*, Measurement of underlying event characteristics using charged particles in pp collisions at $\sqrt{s} = 900$ GeV and 7 TeV with the ATLAS detector, *Phys. Rev. D* **83**, p. 112001 (2011).
8. S. Chatrchyan *et al.*, Measurement of the underlying event in the Drell-Yan

process in proton−proton collisions at $\sqrt{s}$ = 7 TeV, *Eur. Phys. J. C* **72**, p. 2080 (2012).
9. T. Sjöstrand and M. V. Zijl, Multiple parton-parton interactions in an impact parameter picture, *Phys. Lett. B* **188**, p. 149 (1987).
10. L. Frankfurt, M. Strikman and C. Weiss, Transverse nucleon structure and diagnostics of hard parton-parton processes at LHC, *Phys. Rev. D* **83**, p. 054012 (2011).
11. T. Sjöstrand, S. Mrenna and P. Skands, PYTHIA 6.4 physics and manual, *JHEP* **05**, p. 026 (2006).
12. T. Sjöstrand, S. Mrenna and P. Z. Skands, A Brief Introduction to PYTHIA 8.1, *Comput.Phys.Commun.* **178**, p. 852 (2008).
13. M. Bähr, S. Gieseke, M. A. Gigg, D. Grellscheid, K. Hamilton, O. Latunde-Dada, S. Plätzer, P. Richardson, M. H. Seymour, A. Shrestnev and B. R. Webbers, Herwig++ physics and manual, *Eur. Phys. J. C* **58**, p. 639 (2008).
14. T. Sjostrand and P. Z. Skands, Transverse-momentum-ordered showers and interleaved multiple interactions, *Eur. Phys. J. C* **39**, p. 129 (2005).
15. B. Andersson, G. Gustafson, G. Ingelman, and T. Sjöstrand, Parton fragmentation and string dynamics, *Phys. Rept.* **97**, p. 31 (1983).
16. CMS Collaboration, Measurement of energy flow at large pseudorapidities in *pp* collisions at $\sqrt{s} = 0.9$ and 7 TeV, *JHEP* **11**, p. 148 (2011).
17. CMS Collaboration, *Underlying Event Tunes and Double Parton Scattering*, CMS Physics Analysis Summary CMS-PAS-GEN-14-001 (2014).
18. R. Corke and T. Sjöstrand, Interleaved parton showers and tuning prospects, *JHEP* **03**, p. 032 (2011).
19. M. H. Seymour and A. Siodmok, Constraining MPI models using σ_{eff} and recent Tevatron and LHC Underlying Event data, *JHEP* **10**, p. 113 (2013).
20. S. Chatrchyan *et al.*, Description and performance of track and primary-vertex reconstruction with the CMS tracker, *JINST* **9**, p. P10009 (2014).
21. S. Chatrchyan *et al.*, The CMS experiment at the CERN LHC, *JINST* **03**, p. S08004 (2008).
22. J. Pumplin, Hard underlying event correction to inclusive jet cross sections, *Phys. Rev. D* **57**, p. 5787 (1998).
23. V. Khachatryan *et al.*, CMS tracking performance results from early LHC operation, *Eur. Phys. J. C* **70**, p. 1165 (2010).
24. CMS Collaboration, *Performance of Jet Reconstruction with Charged Tracks only*, CMS Physics Analysis Summary CMS-PAS-JME-08-001 (2008).
25. G. P. Salam and G. Soyez, A practical seedless infrared-safe cone jet algorithm, *JHEP* **05**, p. 086 (2007).
26. M. Cacciari, G. P. Salam and G. Soyez, The anti-k_t jet clustering algorithm, *JHEP* **04**, p. 063 (2008).
27. G. D'Agostini, A multidimensional unfolding method based on Bayes' theorem, *Nucl. Instr. Meth. Phys. Res. A* **362**, p. 487 (1995).